

# Toward Stable Solar Hydrogen Generation Using Organic Photoelectrochemical Cells

Marta Haro,<sup>†</sup> Claudia Solis,<sup>†,‡</sup> Gonzalo Molina,<sup>†</sup> Luis Otero,<sup>‡</sup> Juan Bisquert,<sup>†,§</sup> Sixto Gimenez,<sup>\*,†</sup> and Antonio Guerrero<sup>\*,†</sup>

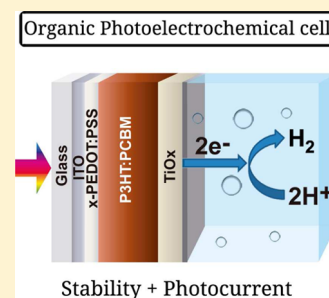
<sup>†</sup>Photovoltaics and Optoelectronic Devices Group, Departament de Física, Universitat Jaume I, Avda. Sos Baynat, s/n, 12071 Castelló, Spain

<sup>‡</sup>Universidad Nacional Rio Cuarto, Departamento de Química, X5804BYA, Río Cuarto, Argentina

<sup>§</sup>Department of Chemistry, Faculty of Science, King Abdulaziz University, Jeddah 21589, Saudi Arabia

## Supporting Information

**ABSTRACT:** Organic photoactive materials are promising candidates for the generation of solar fuels in terms of efficiency and cost. However, their low stability in aqueous media constitutes a serious problem for technological deployment. Here we present organic photocathodes for the generation of hydrogen in aqueous media with outstanding stability. The device design relies on the use of water-resistant selective contacts, which protect a P3HT:PCBM photoactive layer. An insoluble cross-linked PEDOT:PSS hole-selective layer avoids delamination of the film, and an electron-selective TiO<sub>x</sub> layer in contact with the aqueous solution electrically communicates the organic layer with the hydrogen-evolving catalyst (Pt). We developed a novel method for the synthesis of the TiO<sub>x</sub> layer compatible with low-temperature conditions. Tuning the thickness of the TiO<sub>x</sub>/Pt layer leads to a trade-off between the achievable photocurrent ( $\sim 1 \text{ mAcm}^{-2}$ ) and the stability of the photocathode (stable hydrogen generation of  $1.5 \mu\text{mol h}^{-1} \text{ cm}^{-2}$  for  $>3 \text{ h}$ ).



## INTRODUCTION

Photoelectrochemical generation of fuels with semiconductor materials offers a versatile strategy to efficiently capture and store the solar energy incident on the earth crust.<sup>1</sup> One of the most interesting approaches conveys the reduction of water to H<sub>2</sub> or CO<sub>2</sub> to carbon-based molecules. A suitable semiconductor material must satisfy very stringent conditions in terms of cost, efficiency, stability under operating conditions, light absorption in the visible range, and adequate alignment of band edges with the relevant reaction potentials to efficiently carry out these processes.<sup>2</sup> To date, no single material has been identified that encompasses all of these properties, and schemes considering more sophisticated arrangements, like tandem configuration or a PV device connected to a (photo)electrode, are taking the lead in solar hydrogen research.<sup>3</sup> A record 12.3% solar-to-hydrogen efficiency has been recently reported with a metalorganic perovskite tandem configuration coupled to an electrolyzer with earth-abundant catalysts,<sup>4</sup> highlighting the enormous potential of organic and metalorganic materials for solar fuel generation.

In this context, organic materials constitute promising candidates for solar fuels generation due to their synthetic versatility and tunability of optical and electronic properties.<sup>5</sup> Although there has been some interesting studies on the generation of solar fuels with organic materials,<sup>6,7</sup> immersing the photoelectrodes in liquid solutions systematically led to very low photocurrents under application of electrical bias. The stability of the devices has not been studied in detail, rendering

reasonable doubts on the origin of the photocurrent, which could be due to photodegradation effects.

One possible strategy to improve the stability of otherwise highly unstable organic photoelectrodes is using nanometric protective layers, which provide effective electronic communication between the light-absorbing semiconductor material and the catalytic material at the interface with the solution while preserving the structural and functional integrity of the light absorbing semiconductor material. As a relevant recent example, atomic layer deposition of TiO<sub>x</sub> layers on Si, GaAs, and GaP photoanodes led to high performance and high stability of these (unstable) materials under alkaline conditions.<sup>8</sup> Additionally, atomic layer deposition of ZnO and TiO<sub>2</sub> nanometric layers on Cu<sub>2</sub>O photoanodes also led to significantly improved stability of this material under highly acidic conditions.<sup>9</sup>

We have recently shown that interfacing a photovoltaic organic device (bulk heterojunction solar cell) with a liquid medium under illumination provides quantitative extraction of (photo)-carriers for electrochemical reactions at the semiconductor–liquid junction (SCLJ).<sup>10</sup> We showed unprecedented photocurrent of  $4 \text{ mA cm}^{-2}$ , demonstrating that no fundamental limitation at the SCLJ is present for the efficient extraction of carriers. Following this promising result, we

**Received:** February 11, 2015

**Revised:** March 5, 2015

provided the operation principles of organic photoelectrochemical devices (OPECs) by using a model system in nonaqueous electrolyte for the production of fuels. However, this model system was far from a “real” photoelectrochemical cell in which production of hydrogen takes place in aqueous solution. Consequently, in the present study, we focus on the development of stable organic photoelectrodes able to photoreduce protons to H<sub>2</sub>. The organic device is based on a photovoltaic configuration ITO/PEDOT:PSS/P3HT:PCBM, which is illuminated from the substrate (ITO). Carriers are photogenerated at the P3HT:PCBM organic layer, and holes are transported to the hole-selective contact PEDOT:PSS layer, while electrons are driven to the solution to react with protons generating H<sub>2</sub>. Because the direct contact of a biased organic device with the aqueous solution led to negligible photocurrents, we have modified the device architecture combining the integration of a cross-linked PEDOT:PSS (x-PEDOT:PSS) hole selective layer to avoid delamination of the film, with the deposition of an amorphous TiO<sub>x</sub> layer with a hydrogen evolving catalyst (Pt) at the SCLJ for hydrogen evolution to prevent photodegradation of the organic blend.

## MATERIALS AND EXPERIMENTAL METHODS

**Materials.** The following materials were used to prepare OPEC and OPV electrodes: P3HT (Luminescence Technology), PC<sub>60</sub>BM (Solenne, 99.5%), poly(3,4-ethylenedioxy thiophene):polystyrene sulfonic acid (PEDOT:PSS, CLEVIOS P Al 4083), cross-linkable PEDOT:PSS (AGFA, NT5 3442803/2), ITO (PTB7 laboratories, 10 Ω/sq), *o*-dichlorobenzene (Aldrich, 99.9%), calcium (Aldrich, 99.99%), silver (Aldrich, 99.99%), titanium isopropoxide (Aldrich, 97%), ethanol (Panreac PA, absolut), isopropanol (Aldrich, 99.5%), and hydrochloric acid (Sigma-Aldrich, 37%). All materials were used as received without further purification; ethanol and isopropanol were dried over molecular sieves. P3HT:PCBM blends were prepared from dry *o*-dichlorobenzene (1:1, 34 mg/mL) and were stirred at 70 °C for 16 h before sample preparation. For the preparation of the electrolytic solutions, Na<sub>2</sub>SO<sub>4</sub> (Aldrich, 98.0%) and H<sub>2</sub>SO<sub>4</sub> (Fluka, 99.0%) were solved in milli-Q double-distilled water.

**Synthesis of the TiO<sub>x</sub> Layers.** In a glovebox titanium(IV) isopropoxide (TIPT, 150 μL) is added to a mixture ethanol/isopropanol (5:5 mL) to provide a concentration of 0.05 M. The solution is stirred for 5 min, and the closed vial is taken to ambient, where concentrated HCl is added to the solution. The water concentration in the HCl offers a water to TIPT molar ratio of 0.82. The precursor solution is stirred for 72 h at room temperature in the sealed vial.

**Preparation of the Photocathodes and Organic Solar Cells.** Photocathodes were prepared in the configuration ITO/PEDOT:PSS/P3HT:PC<sub>60</sub>BM/TiO<sub>x</sub>/Pt, and optimized configuration is described here. ITO substrates were cleaned and UV-ozone was treated prior to deposition in ambient of PEDOT:PSS by spin coating at 5500 rpm onto film thickness of ~40 nm. The substrate was heated in air at 200 °C for 10 min to promote cross-linking of the PEDOT:PSS. A second thermal treatment was carried out in the glovebox at 130 °C for 10 min to remove traces of water. The P3HT:PCBM blend was deposited at 1200 rpm for 60 s, and the substrate was introduced in a Petri dish and was allowed to dry over a period of 2 h. After this time the active layer was thermally treated at 130 °C for 10 min. The device is taken outside the glovebox. The TiO<sub>x</sub> solution was filtered through a nylon filter (0.45 μm

pore size) and was spin-coated on the substrate or active layer in air at 1000 rpm for 60 s and kept in the ambient at room temperature for 2 h. A thermal treatment at 85 °C for 10 min was observed to be beneficial for the device performance. Thin platinum layers were sputtered by using a BALTEC (SCD 500) sputter coater by using a current of 50 mA for 2–5 s while keeping the distance between Pt source and substrates at ~5 cm at a base pressure of 5 × 10<sup>-3</sup> mbar. This provides a Pt thickness of ~0.5 nm according to the calibration curve provided by the manufacturer. To increase the thickness of the TiO<sub>x</sub>/Pt, successive layers can be carried out without dissolving the underlayers; three spin coating + three sputtering cycles give rise to 140 nm TiO<sub>x</sub> layer, as shown in Figure 2.

Organic photovoltaic devices (OPVs) were fabricated in the configuration ITO/PEDOT:PSS/P3HT:PC<sub>60</sub>BM/TiO<sub>x</sub>/Ag. The main difference in the preparation compared with the photocathode is described here: (1) Prepatterned ITO is used to provide a final active area of 0.25 cm<sup>2</sup>. (2) A thermally evaporated layer of Ag (100 nm) is deposited on the top of the TiO<sub>x</sub>. (3) Devices are encapsulated with a photoresin and a glass microscopy slide.

**Characterization Techniques.** Photoelectrochemical characterization was performed in a three-electrode configuration, where a graphite bar and a Ag/AgCl (KCl, 3M) were, respectively, used as counterelectrode and as reference. The electrolyte was 0.1 M Na<sub>2</sub>SO<sub>4</sub> (acidified to pH 2 with H<sub>2</sub>SO<sub>4</sub>). This pH was selected to attain an optimum compromise between photocurrent and stability. The area of the electrodes was 0.5 cm<sup>2</sup>. The electrodes were illuminated directly through the substrate, while the electrode was in contact with the electrolyte using a 300 W Xe lamp, where the light intensity was adjusted with a thermopile to 100 mW cm<sup>-2</sup>. The light intensity was measured using an optical power meter 70310 from Oriel Instruments, where a Si photodiode was used to calibrate the system. All potentials have been referred to the RHE electrode:  $E_{\text{RHE}} = E_{\text{Ag/AgCl}} + 0.210 + 0.059 \cdot \text{pH}$ . Linear sweep voltammetry (5 mV/s) and chronamperometric measurements (stability tests) were performed with a PGSTAT-30 Autolab potentiostat under chopped light.

For H<sub>2</sub> measurements, a homemade sealed photoelectrochemical cell was used where an Ar stream (~20 mL min<sup>-1</sup>) is constantly flowing through the cell during the measurement as well as the previous 30 min to ensure a complete purge of the system. The electrode is immersed in the solution (0.1 M Na<sub>2</sub>SO<sub>4</sub>, pH 2 with H<sub>2</sub>SO<sub>4</sub>) in the middle of the cell and continuously illuminated (100 mW cm<sup>-2</sup>) to the electrode face with  $V_{\text{bias}} = 0$  V versus RHE in a three-electrode configuration (graphite bar and a Ag/AgCl (KCl, 3M) were the counterelectrode and the reference). The area of the electrode was 0.82 cm<sup>2</sup> defined by an epoxy resin (Loctite 3425 A+B Hysol Epoxy) and determined by image analysis software (ImageJ). The outlet gas is analyzed every 10 min by a chromatograph Agilent Technologies AG-490 (with thermal conductivity detector (μTCD) together with a narrow-bore column).

The photocathodes were characterized by a JEOL JEM-3100F field-emission scanning electron microscope (FESEM). TiO<sub>x</sub> nanoparticles were analyzed by spin coating the nanoparticles solutions using the same conditions as those used for photocathode generation either onto a copper grid for TEM analysis (JEOL 2100) or onto ITO glasses for electrochemical measurements. For X-ray diffraction (Siemens D5000 diffractometer with Cu Kα radiation) the material was deposited by drop-cast onto a glass substrate. Electrochemical character-

ization of the  $\text{TiO}_x$  layers was carried out using a three-electrode configuration in propylene carbonate using  $\text{LiClO}_4$  as electrolyte (0.1M). Pt is used as counterelectrode, Ag/AgCl (3 M KCl) as reference. Thin-film thicknesses were measured by using a Dektak 6 M stylus profiler and confirmed by SEM. Platinum thickness was estimated by using the calibration curve of the equipment provider. Current density–voltage characteristics of photovoltaic devices were carried out under illumination with a 1.5G source ( $1000 \text{ W m}^{-2}$ ) using an Abet Sun 2000 solar simulator. The light intensity was adjusted with a calibrated Si solar cell.

## RESULTS AND DISCUSSION

A scheme of the device configuration used in this work and an illustrative energy diagram are shown in Figure 1. As already

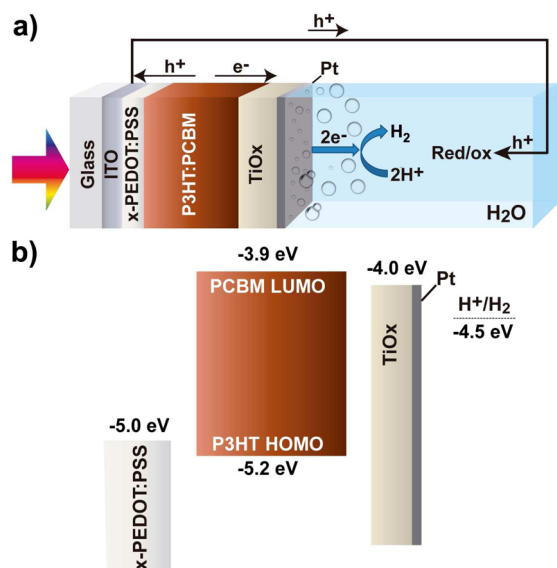
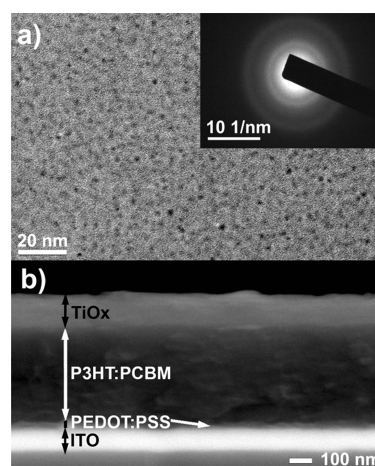


**Figure 1.** (a) Device architecture of the optimized organic photoelectrochemical cell (OPEC) developed in the present study showing the electronic processes taking place during device operation. (b) Energy diagram of the device with literature values measured under vacuum conditions.

mentioned, the photocathodes initially prepared with standard PEDOT:PSS (Al4083) as hole-selective layer showed poor stability during photoelectrochemical characterization due to dissolution of the PEDOT:PSS layer in water and the subsequent delamination of the organic active layer. This is an intrinsic problem because organic polymers, in general, are partially permeable to water.<sup>11</sup> Consequently, a cross-linkable version was used (x-PEDOT:PSS) as an alternative. Comparative images of tested photocathodes with standard and cross-linkable PEDOT:PSS are shown as Supporting Information (Figure SI1). After thermal cross-linking, x-PEDOT:PSS provided insoluble layers in water, which prevents delamination of the organic layer.

Commercially available titania nanoparticles are a common choice as an electron-selective layer in photovoltaic devices;<sup>12</sup> however, these nanoparticles require a high-temperature treatment ( $\sim 500 \text{ }^\circ\text{C}$ ) to attain optimum electronic properties via crystal-phase modification, and this process incompatible with the structural and functional integrity of the organic layer. For this reason, the use of partially oxidized  $\text{TiO}_2$  ( $\text{TiO}_x$ ) nanoparticles has been widely used in organic photo-

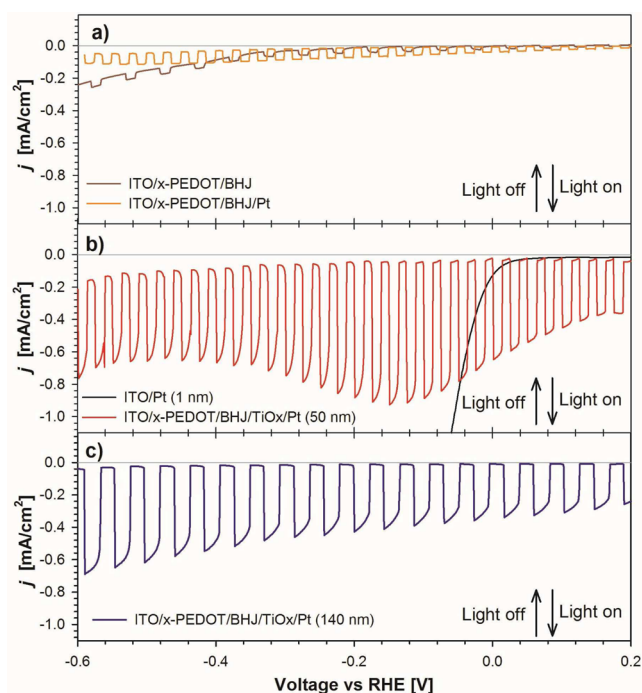
voltaics.<sup>13–15</sup> Initially, we prepared devices with these commercial  $\text{TiO}_2$  nanoparticles using low-temperature processing conditions, but measured photocurrents were negligible (not shown). To solve this problem, we have developed a novel low-temperature process to produce a  $\text{TiO}_x$  layer, which conformably covers the organic blend and enables an adequate electrical contact between this organic layer and the hydrogen evolution catalyst. We used Pt as a model hydrogen reduction catalyst. To obtain a suitable  $\text{TiO}_x$  ink formulation that provides adequate wetting of the organic layer, we modified a previously reported process to include isopropanol in the reaction mixture.<sup>16</sup> Under these conditions, the partial hydrolysis of titanium isopropoxide takes place in the presence of HCl in an ethanol/isopropanol mixture (1:1) at RT. After 72 h of reaction time, the obtained  $\text{TiO}_x$  nanoparticles are highly amorphous with nanoparticle size ranging from 2 to 5 nm, as shown in Figure 2a.



**Figure 2.** (a) Transmission electron microscopy (TEM) micrographs of a thin layer of  $\text{TiO}_x$  nanoparticles. Inset: Diffraction pattern showing that the material is highly amorphous. (b) Cross-section scanning electron microscopy (SEM) image of the most stable device configuration.

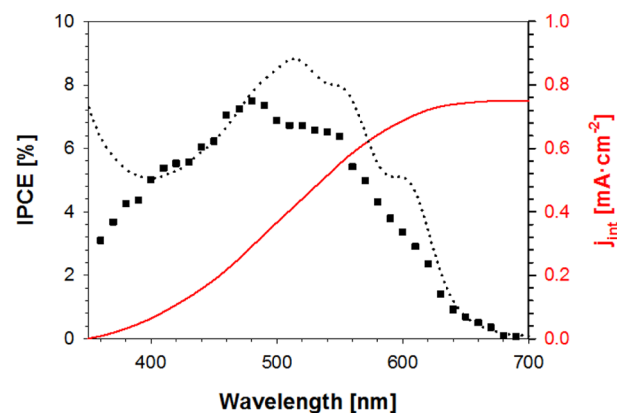
The highly amorphous nature of the  $\text{TiO}_x$  nanoparticulated films prepared in this study is also confirmed by grazing incidence XRD measurements, showing a broad hump between  $20^\circ$  and  $40^\circ$  in the diffraction pattern. (See Supporting Information (SI) Figure SI2.) To validate the suitability of the amorphous  $\text{TiO}_x$  layer for photoelectrochemical generation of hydrogen, we measured the defect density of the material by Mott–Schottky analysis (Figure SI3 in the SI). Interestingly,  $\text{TiO}_x$  synthesized using this method is highly n-doped ( $N_D = 1 \times 10^{20} \text{ cm}^{-3}$ ), showing similar levels of defects as those observed for  $\text{TiO}_2$  thermally treated at  $500 \text{ }^\circ\text{C}$ .<sup>17</sup> This result indicates that although the material is highly amorphous, its conductivity should be adequate for photovoltaic and photoelectrochemical applications. To validate this assumption, we prepared organic photovoltaic devices using  $\text{TiO}_x/\text{Ag}$  and  $\text{Ca}/\text{Ag}$  as electron-selective layers and compared their performance (Figure SI4 in the SI). Although the efficiency using  $\text{TiO}_x/\text{Ag}$  is  $\sim 50\%$  lower compared with the reference devices ( $\text{Ca}/\text{Ag}$ ), the short-circuit currents are comparable (Table SI1 in the SI), which constitutes a very promising result for further evaluation of this material as a photocathode for hydrogen reduction.

Figure 3a shows the  $j$ – $V$  curves measured under chopped illumination for a reference ITO/x-PEDOT/BHJ photo-



**Figure 3.** Linear sweep voltammograms recorded at 5 mV/s in  $\text{Na}_2\text{SO}_4$  0.1 M (pH 2) under chopped illumination for the most promising photocathodes. The basic configuration consists of ITO/P3HT:PCBM/ $\text{TiO}_x$ /Pt. (a) ITO/x-PEDOT/BHJ, ITO/x-PEDOT/BHJ/Pt, (b) ITO/Pt, ITO/x-PEDOT/BHJ/ $\text{TiO}_x$ /Pt (50 nm), and (c) ITO/x-PEDOT/BHJ/ $\text{TiO}_x$ /Pt (140 nm). The scans were carried out by sweeping the applied bias from positive to negative values.  $J = 0$   $\text{mA}/\text{cm}^2$  is indicated with a gray line.

cathode, where BHJ refers to the P3HT:PCBM bulk heterojunction mixture. When a thin layer of 0.5 nm of Pt (which is a model hydrogen evolution catalyst) is deposited on top of the organic layer, the device behaves very similar to the reference photocathode, providing very low photocurrents in the range of  $20 \mu\text{A}/\text{cm}^2$  (Figure 3a). In contrast, when Pt is deposited onto an ITO substrate, the electrode performs as a highly efficient electrocatalyst (Figure 3b). In this case,  $1.4 \text{ mA}/\text{cm}^2$  current is obtained at  $-0.2 \text{ V}$  versus RHE, although it is important to note that this current is originated by the bias applied and not by the effect of the light. These results indicate that there exists a poor electronic connection between the organic layer and the Pt catalyst. A completely different scenario is observed when a  $\text{TiO}_x$  layer (50 nm thick) is placed between the organic layer and the Pt catalyst, providing an optimized configuration as that shown in Figure 1. The  $j$ - $V$  curve under shuttered illumination is shown in Figure 3b. A maximum of  $1 \text{ mA}/\text{cm}^2$  is obtained at about  $-0.1 \text{ V}$  versus RHE, and at  $0 \text{ V}$  versus RHE the photocurrent is  $650 \mu\text{A}/\text{cm}^2$ . A decrease in photocurrent at more negative bias takes place, which was systematically observed for samples delivering the highest photocurrents measured in this study. This effect is probably due to generation of gas bubbles that block the interface  $\text{TiO}_x$ -Pt solution, reducing the active area. The spectral response of the photocurrent was determined by means of IPCE measurements at  $0 \text{ V}$  versus RHE (see Figure 4), and the integrated current is  $700 \mu\text{A}\cdot\text{cm}^{-2}$  in very good agreement with that measured by linear sweep voltammetry. To the best of the authors' knowledge, this result shows an overall 4-fold increase in photocurrent compared with the best



**Figure 4.** IPCE spectrum (squared dots) and integrated current (red solid line) of a representative ITO/x-PEDOT/BHJ/ $\text{TiO}_x$ /Pt (50 nm) device. The absorbance spectrum of the device is also shown (dotted line).

reported results using an OPEC configuration in aqueous solution based on a bulk heterojunction protected by a  $\text{TiO}_2$ / $\text{MoS}_3$  layer.<sup>7</sup> We believe that in this device configuration, the  $\text{TiO}_x$  layer acts as an electron-selective layer for the organic blend; consequently, the present device does not behave as a buried PV+electrolyzer.

When the thickness of the  $\text{TiO}_x$  layer is increased to 140 nm (three deposition cycles), the photocurrent decreases to values around  $350 \mu\text{A}/\text{cm}^2$  at  $0 \text{ V}$  versus RHE. We believe that this is due to the resistive losses associated with this layer, although a significant increase in the device stability is obtained, as discussed later. To assess the resistive losses associated with the  $\text{TiO}_x$  layer, we carried out impedance spectroscopy measurements (SI, Figure S15) on ITO/ $\text{TiO}_x$  samples (140 nm thick) with and without intercalating Pt nanoparticles within the layer under inert electrolyte (acetonitrile, 0.1 M tetrabutylammonium hexafluorophosphate). Large resistances around  $20 \text{ k}\Omega$  at  $0 \text{ V}$  versus RHE are measured for the  $\text{TiO}_x$  layer without intercalated Pt nanoparticles, which are significantly decreased ( $5 \text{ k}\Omega$  at  $0 \text{ V}$  versus RHE) when Pt nanoparticles are incorporated within the layer. We note that intercalating Pt is not the best strategy to enhance the conductivity of the  $\text{TiO}_x$  layer from a practical point of view, and our results must be considered as a first approach toward stable photocathodes.

The obtained photocurrents are significantly lower compared with those from our previous study, where an organic electrolyte with a well-defined redox couple was employed and quantitative photocarrier conversion was achieved.<sup>10</sup> The main reason for the lower values obtained in the present study relates to the higher resistive losses of the water-resistant photoelectrodes and the poorer charge-transfer kinetics in aqueous electrolyte. The dynamics of this chemical reaction is different compared with a one-electron transfer redox reaction. Indeed, the mechanism of hydrogen reduction involves different steps, leading to the injection of two electrons to the solution (electrochemical adsorption and electrochemical or chemical desorption). This entails a kinetic barrier compared with a simple one-electron redox reaction. The open-circuit potential of the tested organic photocathodes was measured, and independently of the thickness of the  $\text{TiO}_x$  layer the obtained value was  $V_{\text{oc}} = 0.47 \text{ V}$  versus RHE, which further validates these organic electrodes for their integration in tandem photoelectrochemical cells.

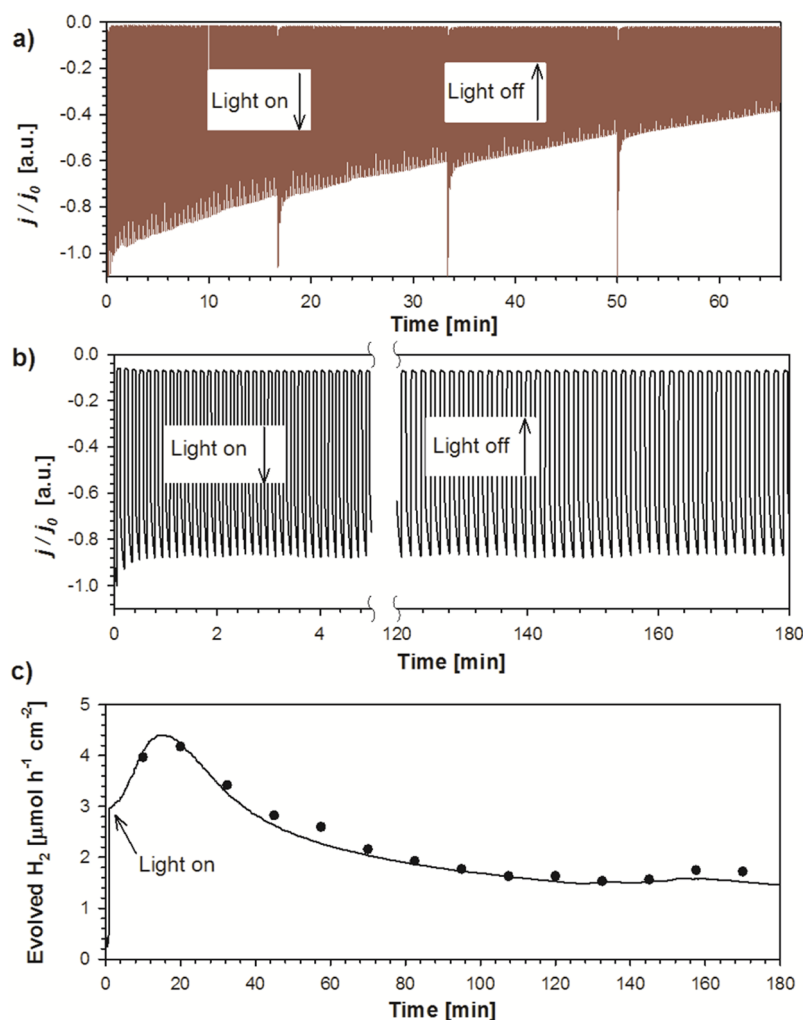


**Figure 5.** (a,b) Normalized chronoamperometry measurements ( $j/j_0$ ) for the configuration glass/ITO/ $x$ -PEDOT:PSS/P3HT:PCBM/TiO<sub>*x*</sub>/Pt in aqueous Na<sub>2</sub>SO<sub>4</sub> (0.1 M, pH 2) under shuttered illumination. (a) Highest photocurrent devices containing a thin layer of TiO<sub>*x*</sub>/Pt (40 nm) measured at 0.15 V versus RHE. (b) Most stable photocathode containing a thick layer of TiO<sub>*x*</sub>/Pt (150 nm) measured at 0 V versus RHE. (c) Hydrogen evolution of the OPEC measured under continuous 1 sun irradiation at 0 V versus RHE registered experimentally (square points) and theoretically calculated from the measured current by the Faraday's law.

The cross section of the device with optimum stability is shown in Figure 2b. The hole-selective layer  $x$ -PEDOT:PSS takes  $\sim 40$  nm, the P3HT:PCBM blend takes 450 nm, and the conformal TiO<sub>*x*</sub>/Pt overlayer takes 140 nm (after three deposition cycles), providing enhanced protection of the organic blend against degradation. We can safely claim that TiO<sub>*x*</sub> does not contribute to the photogeneration of the device because the optical absorbance of devices with and without TiO<sub>*x*</sub> is practically identical, and the IPCE data follow the P3HT:PCBM absorption bands; see Figure SI6 in the SI.

Water and illumination have long been known as two major agents, which promote accelerated degradation of organic photovoltaic devices.<sup>18,19</sup> In particular, the outer contact interfaces are severely affected by the presence of water, leading to contact degradation as well as photo-oxidation of the active layer. For this reason, the stability of an OPEC device in aqueous solution is a major concern. There is only a previous report using a device configuration similar to that employed here, showing an initial photocurrent of  $60 \mu\text{A}/\text{cm}^2$ .<sup>7</sup> In that study, the efficiency decreases 30% in the initial 45 min.

Stability tests were carried out by chronoamperometric measurements (Figure 5) in a three-electrode configuration.

There is a trade-off between achievable photocurrent and the stability of the cathode. Indeed, the photocathode that provides the highest photocurrent (Figure 3b) containing a thin layer of TiO<sub>*x*</sub>/Pt (50 nm) shows poor stability (Figure 5a). A decrease of  $\sim 40\%$  is observed during the first 45 min at 0.15 V (RHE) tested using shuttered light from the initial photocurrent of  $450 \mu\text{A}/\text{cm}^2$ . Absolute photocurrent values are shown as Supporting Information (Figure SI7). When the thin layer of TiO<sub>*x*</sub>/Pt is replaced by a thicker protecting film of 140 nm produced by deposition of three layers of TiO<sub>*x*</sub>/Pt, the stability is significantly enhanced, although this configuration provides more modest photocurrents (Figure 3c). The obtained results at an applied bias of 0 V versus RHE using shuttered light are shown in Figure 5b. Under these conditions, it is observed that the device is totally stable during a period of  $>3$  h from an initial  $250 \mu\text{A}/\text{cm}^2$ . It is important to note that the use of a thicker TiO<sub>*x*</sub> layer introduces a large series resistance in the electron selective layer (Supporting Information, Figure SI5), which is partially responsible for the limited achievable photocurrent but significantly enhances the stability of the photocathode.

The production of H<sub>2</sub> was evaluated by carrying out the chronoamperometric measurements at 0 V versus RHE in a sealed cell under continuous illumination at 100 mW·cm<sup>-2</sup>, and the output gas flow was periodically analyzed by chromatography. Figure 5c shows the evolution of H<sub>2</sub> produced by the organic photocathode under illumination. In this Figure, measured values appear as solid symbols, and the theoretical production of H<sub>2</sub> from the measured photocurrent according to the Faraday's law is also represented (continuous line). The perfect match between the theoretical and experimental data clearly indicates 100% faradaic efficiency. This result confirms that the total extracted photocurrent leads to hydrogen reduction. We note that the chronoamperometric measurement of Figure 5c under continuous illumination exhibits a different shape compared with the behavior shown in Figure 5b under chopped illumination. Under continuous illumination, there is an initial increase in the rate of H<sub>2</sub> production up to 20 min and a subsequent decrease, which stabilizes around 80 min for >100 min at 1.5 μmol·h<sup>-1</sup>·cm<sup>-2</sup>. We believe that the illumination mode is responsible for this different behavior because chopped illumination systematically resulted in increased stability compared with continuous illumination.

## CONCLUSIONS

In summary, we have developed stable organic photoelectrochemical cells for the production of hydrogen in aqueous media. The design relies on the use of an insoluble cross-linkable PEDOT:PSS layer as hole-extracting layer, which prevents delamination, and a TiO<sub>x</sub> layer, which protects the organic blend and electronically communicates the bulk heterojunction and the hydrogen-evolving catalyst. A novel formulation of TiO<sub>x</sub> nanostructured layers with improved wettability on the organic blend compatible with low processing conditions has been developed. The thickness of this layer sets a trade-off between the achievable photocurrent and the stability of the photocathode. An unprecedented performance of 1.6 μmol h<sup>-1</sup> cm<sup>-2</sup> hydrogen generation at 0 V versus RHE for >3 h with a faradaic efficiency of 100% has been achieved for this organic photocathode. These devices take full advantages of organic photovoltaic systems, that is, low production costs<sup>20</sup> or versatility of materials and processing conditions to be used,<sup>21</sup> which highlights the enormous potential of organic materials for solar fuel generation. The present work was focused on approaching toward stable organic hydrogen evolving photocathodes operating under aqueous conditions, and further research is planned to enhance the achieved photocurrents by minimizing the resistivity of the electron selective layer and suppressing the use of noble metals in these structures.

## ASSOCIATED CONTENT

### Supporting Information

Images of electrically tested photocathodes using two different versions of PEDOT:PSS, XRD characterization of TiO<sub>x</sub> nanoparticles, electrochemical characterization of nanoparticles deposited on ITO, *J*-*V* curves of photovoltaic devices using two different electron extraction layers, Nyquist plots of the ITO/TiO<sub>x</sub> samples, absorbance spectra of devices, and not-normalized chronoamperometry measurements. This material is available free of charge via the Internet at <http://pubs.acs.org>.

## AUTHOR INFORMATION

### Corresponding Authors

\*E-mail: [sjulia@uji.es](mailto:sjulia@uji.es).

\*E-mail: [aguerrer@uji.es](mailto:aguerrer@uji.es).

### Notes

The authors declare no competing financial interest.

## ACKNOWLEDGMENTS

We acknowledge financial support from Generalitat Valenciana (ISIC/2012/008 Institute of Nanotechnologies for Clean Energies and PROMETEO 2014/020 FASE II (Disolar)). We acknowledge the financial support of the European Community through the Future and Emerging Technologies (FET) programme under the FP7, collaborative project contract no. 309223 (PHOCS). Serveis Centrals at UJI (SCIC) are acknowledged. We would like to thank Dirk Bollen from Agfa for the supply of x-linkable PEDOT:PSS precursor.

## REFERENCES

- (1) Abdi, F. F.; Han, L.; Smets, A. H. M.; Zeman, M.; Dam, B.; van de Krol, R. Efficient Solar Water Splitting by Enhanced Charge Separation in a Bismuth Vanadate-Silicon Tandem Photoelectrode. *Nat. Commun.* **2012**, *4*, 2195.
- (2) van de Krol, R.; Liang, Y. Q.; Schoonman, J. Solar Hydrogen Production with Nanostructured Metal Oxides. *J. Mater. Chem.* **2008**, *18*, 2311–2320.
- (3) Brillet, J.; Yum, J.-H.; Cornuz, M.; Hisatomi, T.; Solarska, R.; Augustynski, J.; Graetzel, M.; Sivula, K. Highly Efficient Water Splitting by a Dual-Absorber Tandem Cell. *Nat. Photonics* **2013**, *6*, 2012.
- (4) Luo, J.; Im, J.-H.; Mayer, M. T.; Schreier, M.; Nazeeruddin, M. K.; Park, N.-G.; Tilley, S. D.; Fan, H. J.; Graetzel, M. Water Photolysis at 12.3% Efficiency Via Perovskite Photovoltaics and Earth-Abundant Catalysts. *Science* **2014**, *345*, 1593–1596.
- (5) Thompson, B. C.; Frechet, J. M. J. Organic Photovoltaics - Polymer-Fullerene Composite Solar Cells. *Angew. Chem., Int. Ed.* **2008**, *47*, 58–77.
- (6) Esiner, S.; van Eersel, H.; Wienk, M. M.; Janssen, R. A. J. Triple Junction Polymer Solar Cells for Photoelectrochemical Water Splitting. *Adv. Mater.* **2013**, *25*, 2932–2936.
- (7) Bourgeteau, T.; Tondelier, D.; Geffroy, B.; Brisse, R.; Laberty-Robert, C.; Campidelli, S.; de Bettignies, R.; Artero, V.; Palacin, S.; Jusselme, B. A H<sub>2</sub>-Evolving Photocathode Based on Direct Sensitization of Mos3 with an Organic Photovoltaic Cell. *Energy Environ. Sci.* **2013**, *6*, 2706–2713.
- (8) Hu, S.; Shaner, M. R.; Beardslee, J. A.; Lichterman, M.; Brunschwig, B. S.; Lewis, N. S. Amorphous TiO<sub>2</sub> Coatings Stabilize Si, Gaas, and Gap Photoanodes for Efficient Water Oxidation. *Science* **2014**, *344*, 1005–1009.
- (9) Paracchino, A.; Laporte, V.; Sivula, K.; Graetzel, M.; Thimsen, E. Highly Active Oxide Photocathode for Photoelectrochemical Water Reduction. *Nat. Mater.* **2011**, *10*, 456–461.
- (10) Guerrero, A.; Haro, M.; Bellani, S.; Antognazza, M. R.; Meda, L.; Gimenez, S.; Bisquert, J. Organic Photoelectrochemical Cells with Quantitative Photocarrier Conversion. *Energy Environ. Sci.* **2014**, *7*, 3666.
- (11) Tock, R. W. Permeabilities and Water Vapor Transmission Rates for Commercial Polymer Films. *Adv. Polym. Technol.* **1983**, *3*, 223–231.
- (12) O'Regan, B.; Gratzel, M. A Low-Cost, High-Efficiency Solar Cell Based on Dye-Sensitized Colloidal TiO<sub>2</sub> Films. *Nature* **1991**, *353*, 737–740.
- (13) Waldauf, C.; Morana, M.; Denk, P.; Schilinsky, P.; Coakley, K.; Choulis, S. A.; Brabec, C. J. Highly Efficient Inverted Organic

Photovoltaics Using Solution Based Titanium Oxide as Electron Selective Contact. *Appl. Phys. Lett.* **2006**, *89*, 233517–3.

(14) Kim, J. Y.; Kim, S. H.; Lee, H. H.; Lee, K.; Ma, W.; Gong, X.; Heeger, A. J. New Architecture for High-Efficiency Polymer Photovoltaic Cells Using Solution-Based Titanium Oxide as an Optical Spacer. *Adv. Mater.* **2006**, *18*, 572–576.

(15) Guerrero, A.; Chambon, S.; Hirsch, L.; Garcia-Belmonte, G. Light-Modulated TiO<sub>2</sub> Interlayer Dipole and Contact Activation in Organic Solar Cell Cathodes. *Adv. Funct. Mater.* **2014**, *24*, 6234–6240.

(16) Chambon, S.; Destouesse, E.; Pavageau, B.; Hirsch, L.; Wantz, G. Towards an Understanding of Light Activation Processes in Titanium Oxide Based Inverted Organic Solar Cells. *J. Appl. Phys.* **2012**, *112*, 094503.

(17) Kavan, L.; Tétreault, N.; Moehl, T.; Grätzel, M. Electrochemical Characterization of TiO<sub>2</sub> Blocking Layers for Dye-Sensitized Solar Cells. *J. Phys. Chem. C* **2014**, *118*, 16408–16418.

(18) Jørgensen, M.; Norrman, K.; Gevorgyan, S. A.; Tromholt, T.; Andreasen, B.; Krebs, F. C. Stability of Polymer Solar Cells. *Adv. Mater.* **2012**, *24*, 580–612.

(19) Jørgensen, M.; Norrman, K.; Krebs, F. C. Stability/Degradation of Polymer Solar Cells. *Sol. Energy Mater. Sol. Cells* **2008**, *92*, 686–714.

(20) Espinosa, N.; García-Valverde, R.; Urbina, A.; Krebs, F. C. A Life Cycle Analysis of Polymer Solar Cell Modules Prepared Using Roll-to-Roll Methods under Ambient Conditions. *Sol. Energy Mater. Sol. Cells* **2011**, *95*, 1293–1302.

(21) Su, Y.-W.; Lan, S.-C.; Wei, K.-H. Organic Photovoltaics. *Mater. Today* **2012**, *15*, 554–562.